Phase diagram of the spinel oxide MnV_2O_4

Vincent Hardy, Yohann Bréard, and Christine Martin
Laboratoire CRISMAT, ENSICAEN, Université de Caen, CNRS, 6 Bd Maréchal Juin, F-14050 Caen 4, France
(Received 20 May 2008; published 10 July 2008)

Magnetization, susceptibility, and heat-capacity measurements were carried out on MnV_2O_4 ceramic samples. The two main results are as follows: (i) a consistent set of experimental features provides strong support to the existence of two separate transitions in zero-field and (ii) beside the ferrimagnetic transition, the phase diagram in the $H-T$ plane contains two first-order transition (FOT) lines, both connected to the magnetostructural transition temperature in zero field. The new FOT line found at low-H/low-T is discussed in terms of field-induced alignment within the structure of tetragonal domains.

DOI: 10.1103/PhysRevB.78.024406 PACS number(s): 75.50.Gg, 75.25.+z, 75.30.Kz, 75.60.Ej

I. INTRODUCTION

Many of the exotic properties currently investigated in condensed matter (e.g., colossal magnetoresistivity or multiferroic behavior) involve strong couplings between lattice, spins, and orbitals. In particular, it is now widely recognized that the presence of orbital degrees of freedom can play a crucial role.[1] Moreover, it turns out that orbital degeneracy is a feature quite often encountered, as shown, for instance, when considering the common situation of a $3d^n$ transition-metal cation in an octahedral environment; in such a case, the cubic crystal field splits the five $3d$ orbital levels into a high-energy doublet e_g and a low-energy triplet t_{2g}; even if considering only high-spin states, one observes that orbital degeneracy is present in most of the electronic configurations of magnetic $3d^n$ cations, namely, for $n=1,2,4,6,7,9$.

It is well known that strong lattice-orbital coupling takes place when the degeneracy deals with the e_g orbitals (d_{3z2-r2} and d_{x2-y2}). This is at the origin of the pronounced Jahn-Teller (JT) effect encountered, for instance, in Cu^{2+} (e_g^3) and $Mn^{3+}(e_g^1)$, a phenomenon strongly involved in the properties of layered cuprates and magnetoresistive manganites, respectively. Weaker effect are expected for degeneracy on t_{2g} since these orbitals (d_{xy}, d_{yz}, and d_{zx}) do not point directly to the neighboring anions. However, precisely because of such a moderate energy scale, an unusual competition arises between the orbital-lattice coupling and other interactions, such as the spin-orbit, which can generate some exotic behaviors.

One of the best illustration of such a t_{2g} degeneracy is found in the case of octahedrally coordinated V^{3+} ($3d^2:t_{2g}^2$) which is presently the subject of intense activity. Most of the recent studies were focused on two families of oxides: the perovskites RVO_3 (R being a lanthanide),[2–4] in which a transition between two types of orbital ordering plays a crucial role, and the spinels AV_2O_4 (A being a divalent cation),[5–9] in which a complex interplay takes place between the orbital and spin degrees of freedom. The spin degeneracy originates from the fact that the B sublattice in the spinel oxides of general formulation AB_2O_4 form a three-dimensional network of corner-sharing tetrahedra. Provided that the magnetic coupling J_{BB} is antiferromagnetic, the topology of such a so-called pyrochlore lattice leads to very strong effect of geometrical frustration.

With nonmagnetic A cations, this frustration is so prominent in AB_2O_4 compounds that it can impede the setting of long-range ordering down to very low temperatures. However, the presence of orbital degrees of freedom at the B sites can overcome this effect. Indeed, in this case, a structural distortion associated to orbital ordering (OO) can take place, yielding a modulation of the spin-exchange bonds. This effect lifts at least partly the spin degeneracy allowing long-range ordering to set in.[10] Upon cooling ZnV_2O_4, for instance, there is first a cubic-to-tetragonal distortion associated with OO at $T_S \simeq 50$ K, which is followed by antiferromagnetic spin ordering at $T_N \simeq 40$ K.[5,8] Below T_S, at every V^{3+}, one t_{2g} electron occupies the low-energy d_{xy} singlet resulting from tetragonal contraction, while the second electron is distributed on the d_{yz} and d_{zx} orbitals, in a way which is still subject of debate. Several theoretical approaches have been developed for these AV_2O_4 spinels with A=Zn, Mg, and Cd. They primarily differ on the hierarchy which is assumed among the main energy terms in presence, namely, the usual JT effect (orbital-lattice coupling), the effective superexchange (SE) interaction, combining spin and orbital degrees of freedom in a way similar to that first proposed by Kugel and Khomskii,[11] and the relativistic spin-orbit (SO) coupling.

At the present time, the possibility of two types of OO in AV_2O_4 are mainly debated: (i) Combining SE and JT couplings, Tsunetsugu and Motome[12,13] predicted the achievement of an antiferro-orbital ordering, i.e., the stacking of ab planes in which the d_{yz} and d_{zx} orbitals are alternately occupied by the second t_{2g} electron. (ii) Starting from a single-ion picture based on an interplay of SO and JT couplings, Tchernyshyov[14] rather proposed the achievement of a ferro-orbital ordering in which the second electron occupies the same complex ($d_{yz} \pm id_{zx}$) orbital at every V^{3+} sites. This type of OO was also favored by Di Matteo *et al.*[10] in a recent study, putting SO and SE on an equal footing. From an experimental viewpoint, the situation remains controversial, even though the results of recent neutron-scattering experiments were found to be well consistent with the antiferro-orbital ordering.[9,15]

The presence of magnetic A cations in AB_2O_4 can make the situation still more complex. Indeed, if J_{AB} remains moderate enough, the resulting (indirect) BB ferrolike tendency provides a new energy term competing with those discussed above. The spinel which best illustrates this complex interplay is MnV_2O_4. MnV_2O_4 is a so-called normal spinel, in which all tetrahedral A sites are occupied by Mn^{2+} ($3d^5$

yielding $S=5/2$), while the octahedral B sites are occupied by V^{3+} ($3d^2$ for which the large Hund's coupling leads to $S=1$). Because of empty e_g orbitals at the B site, the superexchange coupling J_{AB} is expected to be quite weak.[16] All previous studies devoted to this compound reported that a cubic structure persists over the whole paramagnetic regime, while the ground state is tetragonal ($c<a=b$) and exhibits triangular ferrimagnetism.[17–23,15] This particular magnetic order[24] involves a canting between the V^{3+} spins which yields a resultant moment that is oriented along c and antiparallel to that of Mn^{2+}. The spatial distribution of the ab projections of vanadium moments in this magnetic ordering has been precisely determined in a recent neutron-scattering experiment.[15]

Except a consensus on the above features, several basic questions remain intensively debated, even from a pure experimental point of view. The two main issues are: (i) the way this ground state sets in, namely, via a single magnetostructural transition or through a sequence of two successive transitions and (ii) the influence of the magnetic field on this (these) characteristic temperature(s).

In the early studies, Plumier and Sougi[17] found two distinct transitions: a paramagnetic to collinear ferrimagnetic transition keeping a cubic structure at $T_C=56.25$ K, followed by a second transition to triangular ferrimagnetism accompanied by cubic-to-tetragonal distortion at $T_S=53$ K. Combining x-ray, magnetic, and striction measurements on polycrystalline samples, Adachi *et al.*[18] confirmed this scheme with similar characteristic temperatures ($T_C=56.5$ and $T_S=53.5$ K). Based on the same experimental techniques, however, a second study carried on single crystals[19] claimed the occurrence of a unique $T_S=T_C=57$ K, ascribing these different behaviors to the presence of inhomogeneities in ceramic samples. Recently, the situation was made quite confusing since in another study also performed on single crystals, Zhou *et al.*[20] clearly observed two transitions ($T_C=56$ K and $T_S=52$ K). Even though it is clear that very homogeneous samples are needed owing to the small difference between the two transitions, this study demonstrated that one cannot ascribe a determinant role to the nature of the sample (i.e., single crystalline or polycrystalline).

Beyond this debate on the zero-field behavior, it can be noted that the previous investigations on MnV_2O_4 were not carried out over wide enough temperature- and magnetic-field ranges to build a complete phase diagram in the (H,T) plane. For instance, while heat capacity is known to be well suited for the investigation of phase transitions, this technique was only utilized in quite low magnetic fields (<1 T).[20] In this context, the aim of our work was to reinvestigate the ordering process in MnV_2O_4 by combining magnetic and calorimetric measurements over a wide T range and up to high fields using high quality ceramics.

II. EXPERIMENTAL DETAILS

A batch of polycrystalline MnV_2O_4 samples was prepared by using high-temperature solid-state reaction. Stoichiometric mixture of MnO and V_2O_3 powders was carefully crushed and pressed in the form of bars. These bars were placed in a Pt crucible which was introduced into an evacuated silica ampoule. The synthesis was performed at 1000 °C for 12 h. Samples for transmission electron microscopy (JEOL 200CX) were crushed in butanol to get small flakes which were deposited on a holey carbon film supported by a copper grid. Energy dispersive x-ray spectroscopy coupled to electron diffraction revealed a homogeneous Mn:V ratio, equal to 1:2 within the limit of the technique accuracy. Reconstructing the reciprocal space by tilting around the crystallographic axes confirmed the expected $Fd\bar{3}m$ space group.[17] The room-temperature x-ray pattern was refined in this space group, leading to a cell parameter $a=0.852\,545(5)$ nm which is in line with previous structural data.[17,20]

Magnetization, susceptibility, and heat-capacity measurements were carried out by means of a commercial device (physical properties measurements system, Quantum Design) in magnetic fields up to 9 T. Isothermal $M_T(H)$ curves were recorded after a zero-field cooling from 70 K, a temperature clearly located in the paramagnetic regime. Isofield $M_H(T)$ were recorded either upon cooling or warming, using the so-called field-cooled-cooling (FCC) and field-cooled-warming (FCW) procedures: In practice, the working field H was applied at 70 K, then M was recorded upon cooling down to 5 K (FCC) and subsequently upon warming up to 70 K (FCW). It must be pointed out that FCW is better than the more usual ZFC (zero-field-cooled) mode when investigating hysteretical effects since the global shape of the curves obtained in the latter case can be deeply affected by the uncontrolled residual field present along the "zero-field-cooled" preparation. Magnetic susceptibility was recorded at a frequency of 1000 Hz with an *ac* driving field of amplitude 10 Oe. The heat-capacity curves were registered upon warming from 2 to 300 K using a 2τ relaxation method.

III. RESULTS

A. Measurements in zero field

Figure 1 shows the spontaneous magnetization recorded upon cooling in the remanent field of the magnetometer (<5 Oe). One observes a sudden rise in magnetization at $T\simeq 57$ K which denotes the onset of a magnetic order having a net magnetization. According to the literature, this temperature can be attributed to the transition from paramagnetic to collinear ferrimagnetism (hereafter referred to as T_C). We emphasize that the transition is very sharp—its width (10%–90%) being 0.8 K—which attests to the great homogeneity of this sample. It must also be noted that the curve below T_C exhibits a cusp resulting from a substantial drop in M a few degrees below the maximum. While such a feature can be observed in most of the previous studies on MnV_2O_4, its physical meaning was generally neglected. When T is further decreased below this transition region, M smoothly increases and tends to saturate.

The inset of Fig. 1 shows an enlargement of the out-of-phase *ac* susceptibility curve $\chi''(T)$ recorded in zero dc field. This property related to dissipation is known to be well suited to locate precisely the onset of spontaneous magneti-

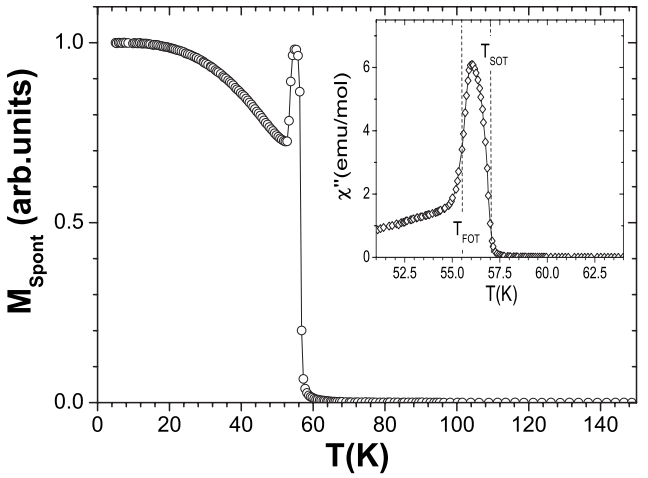

FIG. 1. Spontaneous magnetization of MnV_2O_4. The inset shows an enlargement of the out-of-phase susceptibility (recorded upon warming) in the T range of the transitions. The dashed lines indicate the location of the first-order (T_{FOT}) and second-order (T_{SOT}) transitions derived from low-field magnetization (see text).

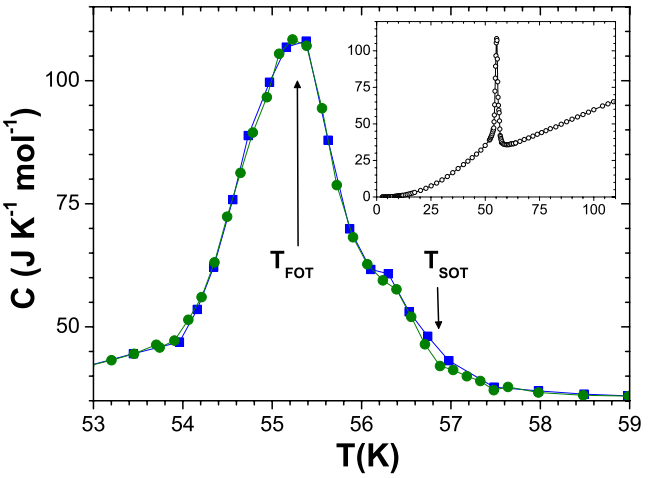

FIG. 3. (Color online) Enlargement of the zero-field heat capacity in the T range of the transitions (the two symbols correspond to two independent set of data). The arrows indicate the location of the first-order and second-order transition temperatures (see text). The inset shows this heat-capacity curve over a wider T range.

zation in ferromagnetic or ferrimagnetic transitions. One observes that χ'' is strictly equal to zero at high T and that it rises suddenly at $T \simeq 57$ K, a temperature in good agreement with that derived from the main panel.

To investigate the presence of hysteresis in the transition region, $M(T)$ curves were recorded in both FCC and FCW modes. We used a field of 25 Oe, a value substantially larger than the remanent field but still small enough not to depart too much from the zero-field conditions. Figure 2 clearly shows the existence of two transitions. The first one at higher temperature corresponds to a magnetization rise as T is decreased. Despite a noticeable field-induced broadening, one observes that the midpoint remains at $\simeq 57$ K, a value consistent with the T_C derived from spontaneous magnetization. More importantly, the perfect superimposition observed between the FCC and FCW curves in this T range demonstrates

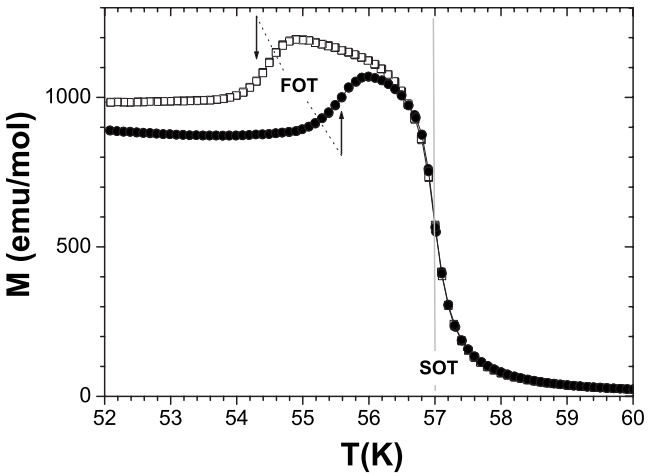

FIG. 2. Low-field (25 Oe) magnetization recorded in the FCC (open squares) and FCW (solid circles) modes. The arrows show the midpoints of a FOT, while the gray line marks the midpoint of a SOT.

the second-order character of this transition, confirming the absence of structural change at T_C. The second transition taking place at lower temperature corresponds to a fall in M as T is decreased. The midpoint of this transition on the FCC and FCW curves is $T^*_{\downarrow}=54.5$ and $T^*_{\uparrow}=55.5$ K, respectively. Such a clear hysteresis is typical of a first-order transition (FOT). One also observes that the value obtained upon cooling is in good agreement with the inflection point of the drop found in spontaneous magnetization. At still lower T (not shown in Fig. 2), the FCC and FCW curves merge on each other and recover a shape similar to that shown in Fig. 1.

The heat capacity of MnV_2O_4 recorded in zero field is shown in Fig. 3. The inset exhibits the presence of a large and sharp peak in the region of the magnetic transitions, while no other feature can be detected out of this T range. In the main panel which displays an enlargement of the transition region, one can clearly observe the presence of a shoulder on the high-T side of the large peak. The good superimposition observed between two independent data sets attests to the reliability of this feature. We notice that such a global shape of the heat-capacity anomaly can be accounted for by considering the presence two transitions whose signatures add to each other: a symmetrical high peak at low-T and a smaller λ-shaped peak centered at a slightly higher T. Because of the overlap between the signatures of these two transitions, only the high-T side of the latter is clearly visible (negative C vs T slope). In this picture, the symmetrical large peak can be ascribed to a FOT centered at the maximum, i.e., $T_{FOT}=55.2$ K, while the second feature is consistent with a second-order transition (SOT). In the latter case, the characteristic temperature must be associated to the inflection point on the high-T side of the λ anomaly,[25] leading to $T_{SOT} \simeq 56.8$ K. We emphasize that these transition temperatures obtained from heat capacity are well consistent with those derived from magnetic measurements, i.e., $T_{SOT} \simeq T_C$ and $T_{FOT} \simeq T^*_{\uparrow}$.

B. Measurements in magnetic field

Series of $M_T(H)$ and $M_H(T)$ curves were recorded over wide H and T ranges (0–9 T and 5–70 K, respectively), while $C_H(T)$ curves were registered in 0, 2, 5, and 9 T from 2 up to 300 K. Figure 4 deals with the most prominent transition line which emerged from this set of data. Isothermal $M_T(H)$ recorded at several temperatures between 52.5 and 62.5 K is shown in Fig. 4(a). While curves at the boundaries of this T range are well reversible, those corresponding to intermediate T show the development of a *bubblelike* hysteresis around a characteristic field which is shifted to higher values as T is increased. A closer look at each branch of the $M_T(H)$ cycles reveals that this anomaly stems from a smoothed upward step in M as H is increased; the hysteresis resulting from the fact that the characteristic field of this step is higher on the field-increasing branch than on the reverse leg (e.g., at 57 K, the inflection points correspond to 3.4 and 1.6 T, respectively).

Related features are clearly visible in the $M_H(T)$ curves shown in Fig. 4(b). In this case, the transition corresponds to a decrease in M as T is increased. We observe that the characteristic temperature is shifted to higher values as H is increased and is larger on the FCW branches than on the FCC ones. There is very good correspondence between the (H,T) couples, marking this transition on either the $M_H(T)$ or $M_T(H)$ curves. For instance, the transition in 2 T derived from $M(T)$ is found to be around 57 K, a temperature for which the hysteretical region in $M(H)$ actually contains the field of 2 T. The pronounced hysteresis found in both $M_T(H)$ and $M_H(T)$ curves provides evidence of the first-order character of this transition. Therefore, there is a slight shift in the exact location of the transition line, depending on the direction of the parameter change. Note that the points derived from the field-decreasing branches of the $M(H)$ curves were found to correspond to those derived from the FCW curves of $M(T)$ [similar equivalence exists between the field-increasing branches in $M(H)$ and the FCC $M(T)$ curves]. Location of this dual line, hereafter referred to as $T^*(H)$, is reported in Fig. 7. Figure 4(c) shows that the heat-capacity data are well consistent with magnetization about the field dependence of this FOT. Not only the location of the large peak is clearly shifted to higher temperatures as H is increased but a direct comparison of Figs. 4(b) and 4(c) also exhibits very good quantitative agreement between the $T^*(H)$ in either magnetic or calorimetric data.

Figure 5(a) shows FCC and FCW curves recorded from 5 to 70 K in 1 T. In this wide T range, one observes the existence of two anomalies accompanied by hysteresis, located around 56 and 37 K. The one at higher T is of same nature as those shown in Fig. 4 and belongs to the $T^*(H)$ line. In contrast, the second transition at lower T corresponds to an increase in M as T is increased. This magnetization step takes place at higher T for FCW than for FCC, leading to a pronounced hysteresis indicative of its first-order nature. In Fig. 5(b), it is shown that the characteristic temperature of this transition decreases as the field is increased. We note that this feature is no longer visible for $H>2$ T.

Although less spectacular, related anomalies are also present on the $M_T(H)$ curves. As shown in Figs. 5(c) and 5(d), one can indeed detect a change in the slope of these curves (a maximum in dM/dH). At a given temperature, the characteristic field associated to this inflection point is larger on the field-increasing branch than on the field-decreasing

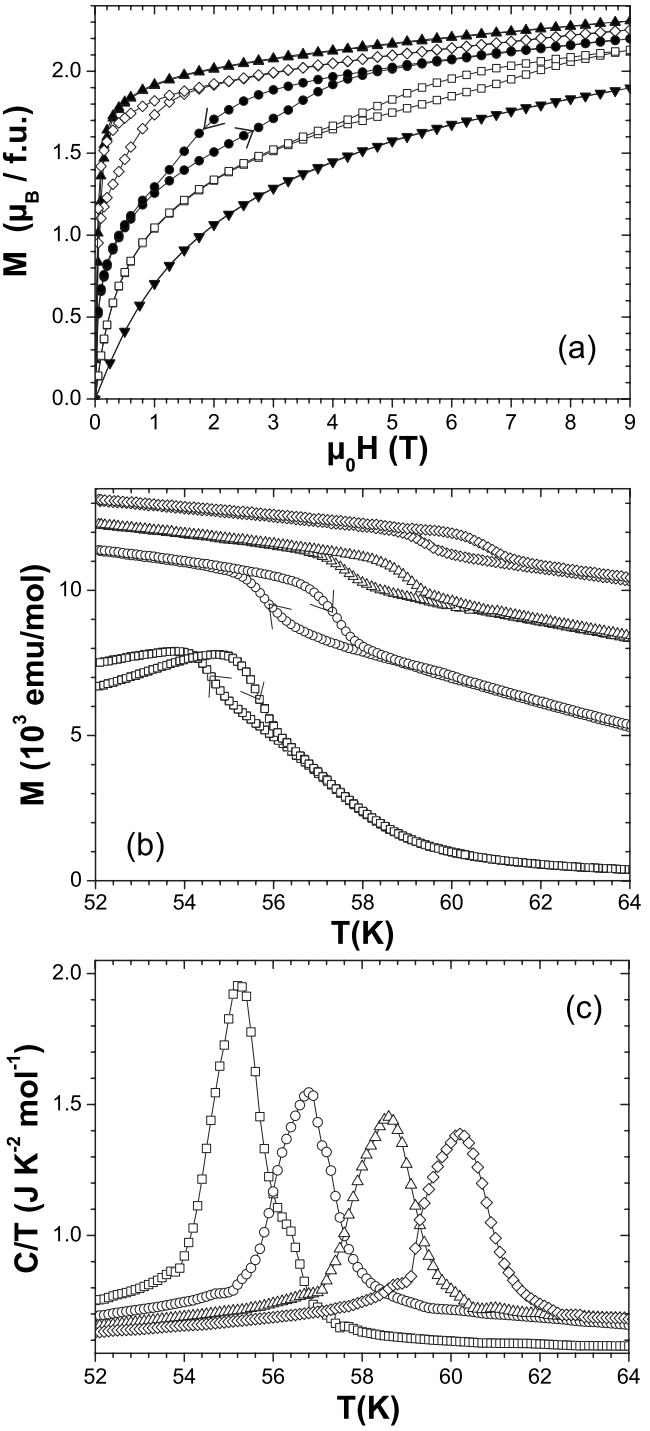

FIG. 4. (a) $M_T(H)$ curves at five temperatures (from top to bottom): 52.5, 55, 57, 59, and 62.5 K. The arrows on the curve at 57 K indicate the direction of the field variation. (b) $M_H(T)$ curves recorded in four field values (from bottom to top): 0.1, 2, 5, and 9 T. The arrows indicate the direction of the temperature variation. (c) $[C_H/T](T)$ curves recorded in four field values (from left to right): 0, 2, 5, and 9 T.

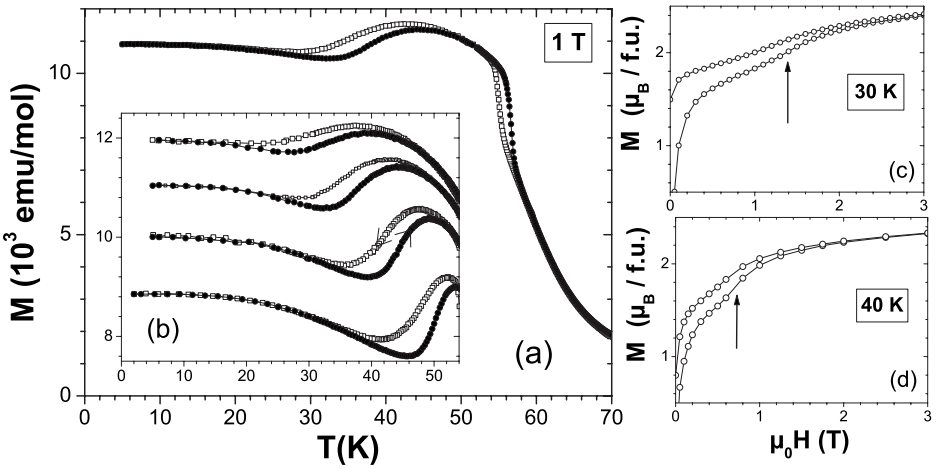

FIG. 5. (a) $M_H(T)$ curves recorded in 1 T upon cooling (open squares) and upon warming (solid circles). Inset (b) shows an enlargement around the low-T transition in various fields (from bottom to top): 0.2, 0.5, 1, and 1.5 T; the arrows indicate the direction of the T variation on one of these curves. The right panels show $M_T(H)$ curves recorded at (c) 30 K and (d) 40 K; the arrows highlight the increase in slope observed on the field-increasing branch of these curves.

one. Comparing Figs. 5(c) and 5(d) also shows that these characteristic fields decrease as T is increased. We note that this signature on the $M_T(H)$ curves is present down to 5 K, while it becomes hardly detectable for $T>45$ K. As for the previous FOT, there is good agreement between the (H,T) couples, marking the transition on either the $M_H(T)$ or $M_T(H)$ curves. For instance, the $M(T)$ curves in 1 T shows the development of hysteresis between 30 and 40 K, temperatures for which the $M(H)$ curves reveal transitions that are slightly above and below 1 T, respectively. The location of this second FOT line, hereafter referred to as $T^{**}(H)$ is reported in Fig. 7. It must be emphasized that the hysteresis of the $M_T(H)$ curves extends down to zero field, showing that this new FOT transition is not completely reversible, contrary to the first one [see Fig. 4(b)].

Finally, we aimed to investigate the field dependence of the ferrimagnetic transition at T_C, keeping in mind that such a transition toward a phase having a spontaneous magnetization becomes ill-defined in magnetic fields. Accordingly, the $T_C(H)$ line we derive below should just be regarded as an evaluation of how much the application of magnetic field can assist—via the Zeeman energy—the achievement of the ferrimagnetic ordering. In low H, we have shown that T_C can be tracked by criteria such as the midpoint increase in $M(T)$ or the appearance of nonzero χ''. Nevertheless, we found that the field broadening is too large that none of these methods is applicable for H larger than about 200 Oe.

Another strategy sometimes used to evaluate $T_C(H)$ consists in inspecting the susceptibility curves $\chi'(T)$ measured in magnetic fields.[26,27] Figure 6 shows that the application of dc fields considerably reduces the susceptibility and splits the $\chi'(T)$ curves, yielding two maxima. As discussed by Baek *et al.*,[23] the maximum at higher temperature can be ascribed to T_C, while the second one corresponds to the Hopkinson effect.[28] This effect is a common feature of ferromagnetic or ferrimagnetic materials (including spinel oxides),[29] which generates a peak in $\chi'(T)$ just below T_C in zero field. Although its exact origin is still a subject of controversy, it is generally ascribed to a crossover in the dynamics of the domain structure (e.g., walls displacements or rotational processes).[30] Under magnetic field, the Hopkinson peak shifts to low T and falls off, which allows a second maximum at $T_C(H)$ to be revealed.[20,27] In moderate fields (e.g., 100 Oe in our case), we observed a good agreement between the location of this high-T maximum in $\chi'(T)$ and the midpoint of $M(T)$. The $T_C(H)$ line derived from the $\chi'_H(T)$ curves is reported in Fig. 7.

In principle, T_C should also be reflected in $C_H(T)$, even though the field-induced broadening can make it hardly detectable. On the high-T side of the large peaks in $C_H(T)$, we observed that the curves remain shifted from the zero-field one [see Fig. 4(c)] over a T range whose width increases with H. Considering for instance the case of $H=2$ T, the inset of Fig. 6 shows an enlargement of the difference $\Delta C(T)=C_{2T}(T)-C_{0T}(T)$ which allows us to better focus on this behavior by discarding the lattice contribution. For $T>59$ K—which corresponds to the high-T foot of the large $C(T)$ peak in 2 T—$\Delta C(T)$ exhibits a shape resembling the high-T side of a λ-shaped anomaly. The midpoint of the T range over which ΔC goes to zero yields a characteristic temperature of ≈67 K which turns out to be well consistent with the high-T maximum of $\chi'(T)$ in 2 T. This good correspondence lends additional support to the reliability of the $T_C(H)$ line derived from $\chi_H(T)$.

The phase diagram of Fig. 7 displays the three transition lines we detected: $T^*(H)$, $T^{**}(H)$, and $T_C(H)$. One of the

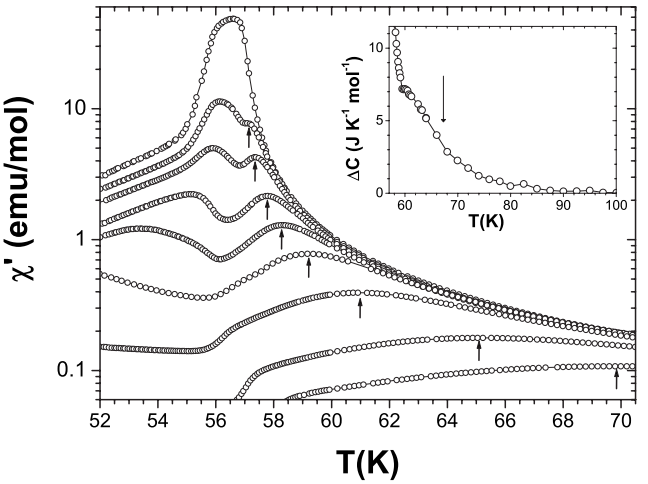

FIG. 6. Semilogarithmic plot of the T dependence of the in-phase susceptibility measured in various fields (from top to bottom): 0, 0.01, 0.02, 0.05, 0.1, 0.2, 0.5, 1.5, and 3 T. The inset shows an enlargement of $\Delta C(T)=C_{2T}(T)-C_{0T}(T)$ (see text).

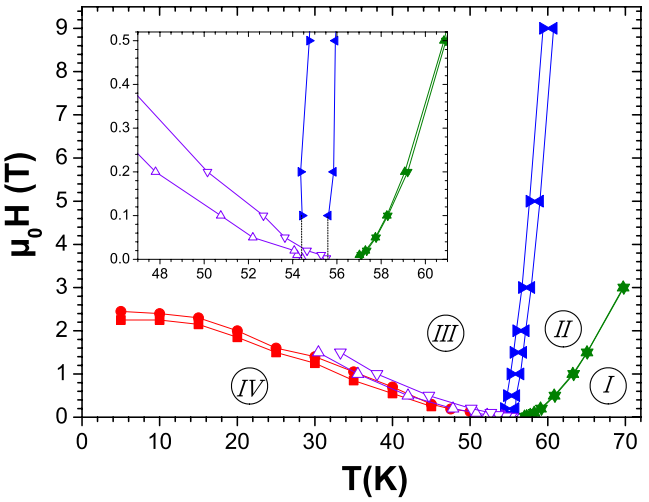

FIG. 7. (Color online) Phase diagram of MnV_2O_4. The $T_C(H)$ line between regions I and II is derived from $\chi'_H(T)$ curves, recorded either upon cooling (solid up triangles) or warming (solid down triangles). The $T^*(H)$ line between regions II and III is derived from $M_H(T)$ curves recorded either upon cooling (solid right triangles) or warming (solid left triangles). The $T^{**}(H)$ line between regions III and IV is derived from the field-increasing (solid circles) or the field-decreasing branches (solid squares) of $M_T(H)$ curves. Additional data points were extracted from $M_H(T)$ curves, recorded either upon cooling (open up triangles) or warming (open down triangles). The inset shows an enlargement in the low-field range. The dashed lines emphasize the merging between the $T^*(H)$ and $T^{**}(H)$ lines in zero field.

main problem encountered when building the phase diagram was the connection between these three lines and the two characteristic temperatures found in zero field. This is made particularly difficult not only by the proximity between these two temperatures but also by the first-order nature of $T^*(H)$ and $T^{**}(H)$ which leads to two slightly shifted lines for each of them. Enlargement of the phase diagram displayed in the inset of Fig. 7 shows a better insight into this issue. Taking into account the direction of the parameter change (i.e., T or H), one observes that both FOT line actually connect to $T^*(H=0)$. For instance, as H is progressively decreased, both the $T^*(H)$ and $T^{**}(H)$ lines derived from FCW data merge onto the value $T^*_\uparrow(0) \simeq 55.5$ K obtained upon warming in 25 Oe (see Fig. 2). The same concordance also exists for the data measured upon cooling. Basically, one is thus dealing with two characteristic temperatures in zero field from which emerge three transition lines, delineating four regions in the $H-T$ plane. The nature of each of these phases is discussed Sec. IV.

IV. DISCUSSION

A. Measurements in zero field

Controversial results were reported in the literature about the existence of only one or two transition temperatures in MnV_2O_4. The present study clearly supports the latter picture with two distinct temperatures: a SOT marking the onset of collinear ferrimagnetic ordering at $T_C \simeq 57$ K and a FOT associated with structural distortion accompanied by spin canting, taking place at $T^*_\downarrow = 54.5$ and $T^*_\uparrow = 55.5$ K upon cooling or warming, respectively. These features derived from magnetization were found to be well consistent with the heat-capacity data.

The existence of such a two-step process contradicts a recent study which claimed the existence of only one transition. Suzuki *et al.*[19] were led to this conclusion by the coincidence they found between the temperature of magnetic ordering derived from $M(T)$ and the temperature of structural transition derived from x-ray data. As a general rule, we emphasize that comparing transition temperatures derived from different properties and measured with different devices can be a delicate task, especially when dealing with a very narrow T interval since all experimental uncertainties are critical in such a case (e.g., calibration of the thermometers, criteria chosen to locate these characteristic temperatures, etc). It is clear that analyzing a unique data curve avoids these difficulties and can lead to less ambiguous conclusions. In this respect, it deserves to be noted that a fall in M just below T_C is present on the $M(T)$ curves of Ref. 19, a feature shown herein to be indicative of a second transition.

Another point of debate emerges about the heat-capacity data. Even though our $C(T)$ curve reveals two transitions as previously reported by Zhou *et al.*,[20] the observed features are profoundly different. In Ref. 20, the peak at low T (corresponding to the structural distortion) is much smaller than the peak at high-T (corresponding to the onset of collinear ferrimagnetism) which is just in odds with our results. First, we argue on general grounds that it is quite unexpected that the peak of a first-order magnetostructural transition is smaller than the one of a purely magnetic second-order transition. Second, we take note that the large peak of $C(T)$—that we attribute to the structural transition—is similar to that found at high T in the AV_2O_4 compounds with nonmagnetic A,[6,31,32] a result consistent with the fact that the same type of OO involving the t_{2g} of V^{3+} is expected in all these vanadates spinels. Furthermore, the integration of C/T over the large peak of Fig. 3 leads to an entropy change of about 3 J/mol K which is well in line with the values reported in ZnV_2O_4 and MgV_2O_4.[6,31,13]

B. Measurements in magnetic field

The FOT line $T^*(H)$ is in good qualitative agreement with the first results of the literature.[17,18] Quantitatively, if one considers dT^*/dH for $H<5$ T, we obtained 0.76 K/T, in reasonable agreement with the previous values: 0.48 K/T (Ref. 17) and 0.66 K/T.[18] On the other hand, our results are in striking contrast with the behavior reported by Zhou *et al.*[20] in which the magnetostructural transition line is claimed to disappears in field $H>0.3$ T. These conclusions being based on the analysis of $C_H(T)$ curves, this disagreement is probably another manifestation of the problems already discussed about heat-capacity data in zero field. We suggest that such a global discrepancy may arise from experimental problems inherent to the derivation of $C(T)$ from a relaxation technique when investigating a first-order transition.[33]

The field dependence of T_C was previously addressed in Refs. 17 and 20. Still for the same reasons, our results are very different from those of Zhou *et al.*[20] in which $T_C(H)$ was derived from the field dependence of the large peak in $C_H(T)$ (while this feature is associated to T^* in our case). Our results also differ from the behavior proposed by Plumier and Sougi[17] in which the collinear ferrimagnetic state in the $H-T$ plane is delineated by a vertical line at $T_C(H=0)$ and an horizontal line at 4 T (a field marking a crossover in the amplitude of the hysteresis at the magnetostructural transition). We found no evidence for such a crossover field and we argue that positive dT_C/dH should be expected since one is dealing with a magnetic order having a nonzero net magnetization. Importantly, dT_C/dH is much smaller than dT^*/dH, which shows that a ferrimagnetic order sets in before the structural transition, whatever the field value.

The second FOT line found at low T was not reported before. First, one can think of a rearrangement of spins in the triangular ferrimagnet, e.g., the appearance of a canting between the A spins.[34] Such a possibility would be reasonable owing to the presence of a substantial antiferromagnetic J_{AA} interaction, as revealed by the high Néel temperature $T_N=40$ K observed in $MnAl_2O_4$.[35] Nevertheless, no indication of such a magnetic transition was detected in the neutron-diffraction studies reported to date. An alternative possibility to interpret this $T^{**}(H)$ line is to consider the structure of ferrimagnetic domains. The importance of this feature was early emphasized by Plumier and Sougi[17] who attributed the remanence observed on the $M(H)$ at low T to the pinning of Bloch walls. More recently, this issue was precisely reinvestigated by Suzuki *et al.*[19] by examining the evolution of Bragg peaks as a function of the field. In zero field, they found the emergence of a multidomains structure at the cubic-to-tetragonal transition, manifested by a threefold splitting of the Bragg peaks. As the field is increased, some of these peaks disappear, the only remaining peaks in large fields being those corresponding to domains having their c axis oriented along the magnetic field. Suzuki *et al.*[19] proposed that such a magnetic-field-induced alignment of tetragonal domains might play a role in the large anisotropic magnetostriction they observed at low T.

We suggest that the $T^{**}(H)$ line might be another manifestation of this phenomenon. As the field is increased, the Zeeman term can induce a rotation of the c axis in some tetragonal domains in order to make their magnetization being oriented along the field direction. The strains resulting from such changes in the domain structure might confer on this transition its first-order nature. Several experimental features would support such a picture: (1) Both $M(H)$ and $M(T)$ curves show that the magnetization in larger in region III than in region IV. (2) A large peak emerge on the $\chi''_H(T)$ curves recorded in magnetic fields (not shown), in agreement with the expected dissipation resulting from a reorganization in a domain structure. The location of this peak on $\chi''_H(T)$ curves well follows the $T^{**}(H)$ line. For instance, it is found at 51 K in 0.2 T and shifts to 38 K in 1 T. (3) No anomaly was detected on the $C_{2T}(T)$ curve around $T^{**}(2T)$, as expected for a transition involving only the domain structure. Finally, we point out that the T dependence of the crossover field present on the magnetostriction curves at low-T reported in Ref. 19 is very close to that of the $T^{**}(H)$ line.

In conclusion, our picture about the different phases found in the $H-T$ plane is as follows: (I) Paramagnetic regime with a cubic structure, (II) cubic ferrimagnet (collinear ordering), (III) tetragonal ferrimagnet (triangular ordering) with domains mainly oriented along the magnetic field, and (IV) tetragonal ferrimagnet (triangular ordering) with unoriented domains. We emphasize that in transition III/IV showing a large hysteresis (especially versus field), the state of the system around this line depends a lot on the magnetothermal history.

V. CONCLUSION

A combined analysis of magnetic and heat-capacity measurements in MnV_2O_4 clearly demonstrates that the ordering process in zero field takes place in two steps. The first transition taking place at $T_C(0)=57$ K is a SOT from paramagnetic to collinear ferrimagnetic regimes, keeping the cubic structure. It can be regarded as the standard spin ordering driven by the J_{AB} interaction in spinel oxides of general formula AB_2O_4. The second transition at lower T is a magnetostructural FOT driven by an OO at the B sites. It occurs upon warming at $T^*_{\uparrow}(0)=55.5$ K and upon cooling at $T^*_{\downarrow}(0)=54.5$ K. This ordering of the t_{2g} orbital of V^{3+} implies tetragonal distortion which in turn allows the triangular ferrimagnetic configuration to set in. Indeed, this spin ordering—that is, the expected ground state in the presence of antiferromagnetic J_{AB} and J_{BB} interactions[24]—is unstable in cubic symmetry whereas it can take place in tetragonal symmetry.[34] We note that the existence of a two-step ordering process in zero field is consistent with the conclusions of a very recent neutron-diffraction investigation.[15]

Upon application of magnetic field, the ferrimagnetic collinear state extents to higher temperatures (large positive dT_C/dH slope), while two FOT lines emerge from $T^*(0)$. The one at higher T (small positive dT^*/dH slope) corresponds to the magnetostructural transition from cubic/collinear to tetragonal/triangular ferrimagnetism. Its field dependence results from a strong interplay of spin and orbital orderings. Following the idea of Adachi *et al.*,[18] the following mechanism is proposed: (1) the presence of a collinear ferrimagnetic state induces an effective ferromagnetic coupling within the V^{3+} sublattice; (2) through the SE interaction, this ferromagnetic spin-coupling favors an antiferromagnetic orbital coupling within the t_{2g} orbitals of V^{3+}; (3) this orbital coupling, assisted by the JT effect, induces an OO with tetragonal distortion; and (4) this structural distortion stabilizes a canting within the V spins leading to the triangular ferrimagnetic order. The application of magnetic fields favors the collinear ferrimagnetic state which shifts the whole process toward higher T. Due to the field-independent energy scale of the JT effect, however, dT^*/dH is much smaller than dT_C/dH.

The second FOT we observed in the phase diagram of MnV_2O_4 has a negative dT^{**}/dH slope. We tentatively ascribe this new line to a phenomenon of field-induced alignment within the structure of tetragonal domains. The resulting development of strains at the interfaces between domains

might generate the observed first-order character of this transition. However, a striking feature of this transition is its persistence in $M(T)$ measured upon cooling in quite large fields (FCC mode). Such an observation seems hardly compatible with a picture in which the c axis of all tetragonal domains would be aligned in large fields. It suggests that other processes such as flipping of the magnetization away from the c axis may also be in play at the $T^{**}(H)$ line. Clearly, the origin of this new FOT line at low T/low H will deserve further investigations. In particular, single-crystal neutron diffraction in magnetic field would be highly welcome.

ACKNOWLEDGMENTS

The authors acknowledge the financial support of the "Programme Interdisciplinaire ENERGIE" of CNRS (France) for this project.

[1] P. G. Radaelli, New J. Phys. **7**, 53 (2005).
[2] G. R. Blake, T. T. M. Palstra, Y. Ren, A. A. Nugroho, and A. A. Menovsky, Phys. Rev. Lett. **87**, 245501 (2001).
[3] S. Miyasaka, Y. Okimoto, M. Iwama and Y. Tokura, Phys. Rev. B **68**, 100406(R) (2003).
[4] J.-Q. Yan, J.-S. Zhou, J. B. Goodenough, Y. Ren, J. G. Cheng, S. Chang, J. Zarestky, O. Garlea, A. Liobet, H. D. Zhou, Y. Sui, W. H. Su, and R. J. McQueeney, Phys. Rev. Lett. **99**, 197201 (2007).
[5] Y. Ueda, N. Fujiwara, and H. Yasuoka, J. Phys. Soc. Jpn. **66**, 778 (1997).
[6] H. Mamiya, M. Onoda, T. Furubayashi, J. Tang, and I. Nakatani, J. Appl. Phys. **81**, 5289 (1997).
[7] N. Nishiguchi and M. Onoda, J. Phys.: Condens. Matter **14**, L551 (2002).
[8] M. Reehuis, A. Krimmel, N. Büttgen, A. Lloid, and A. Prokofiev, Eur. Phys. J. B **35**, 311 (2003).
[9] S.-H. Lee, D. Louca, H. Ueda, S. Park, T. J. Sato, M. Isobe, Y. Ueda, S. Rosenkranz, P. Zschack, J. Íñiguez, Y. Qiu, and R. Osborn, Phys. Rev. Lett. **93**, 156407 (2004).
[10] S. Di Matteo, G. Jackeli and N. B. Perkins, Phys. Rev. B **72**, 020408(R) (2005).
[11] K. I. Kugel, and D. I. Khomskii, Zh. Eksp. Teor. Fiz. **64**, 369 (1973)[Sov. Phys. JETP **37**, 725 (1973)].
[12] H. Tsunetsugu and Y. Motome, Phys. Rev. B **68**, 060405(R) (2003).
[13] Y. Motome and H. Tsunetsugu, Phys. Rev. B **70**, 184427 (2004).
[14] O. Tchernyshyov, Phys. Rev. Lett. **93**, 157206 (2004).
[15] V. O. Garlea, R. Jin, D. Mandrus, B. Roessli, Q. Huang, M. Miller, A. J. Schultz, and S. E. Nagler, Phys. Rev. Lett. **100**, 066404 (2008).
[16] D. G. Wickham and J. B. Goodenough, Phys. Rev. **115**, 1156 (1959).
[17] R. Plumier and M. Sougi, Solid State Commun. **64**, 53 (1987); Physica B **155**, 315 (1989).
[18] K. Adachi, T. Suzuki, K. Kato, K. Osaka, M. Takata, and T. Katsufuji, Phys. Rev. Lett. **95**, 197202 (2005).
[19] T. Suzuki, M. Katsumura, K. Taniguchi, T. Arima, and T. Katsufuji, Phys. Rev. Lett. **98**, 127203 (2007).
[20] H. D. Zhou, J. Lu, and C. R. Wiebe, Phys. Rev. B **76**, 174403 (2007).
[21] N. B. Perkins and O. Sikora, Phys. Rev. B **76**, 214434 (2007).
[22] J.-H. Chung, J.-H. Kim, S.-H. Lee, T. J. Sato, T. Suzuki, M. Katsumura, and T. Katsufuji, Phys. Rev. B **77**, 054412 (2008).
[23] S.-H. Baek, K.-Y. Choi, A. P. Reyes, P. L. Kuhns, N. J. Curro, V. Ramanchandran, N. S. Dalal, H. D. Zhou, and C. R. Wiebe, J. Phys.: Condens. Matter **20**, 135218 (2008).
[24] Y. Yafet and C. Kittel, Phys. Rev. **87**, 290 (1952).
[25] S. Yu. Dan'kov, A. M. Tishin, V. K. Pecharsky, and K. A. Gschneidner, Phys. Rev. B **57**, 3478 (1998).
[26] X. Z. Zhou, H. P. Kunkel, J. H. Zhao, P. A. Stampe, and G. Williams, Phys. Rev. B **56**, R12714 (1997).
[27] G. Ehlers, C. Ritter, J. R. Stewart, A. D. Hillier, and H. Maletta, Phys. Rev. B **75**, 024420 (2007).
[28] J. Hopkinson, Philos. Trans. R. Soc. London, Ser. A **180**, 443 (1889).
[29] P. A. Joy and S. K. Date, J. Magn. Magn. Mater. **210**, 31 (2000); **218**, 229 (2000).
[30] G. L. Ferreira-Fraga, L. A. Borba, and P. Pureur, Phys. Rev. B **74**, 064427 (2006).
[31] S. Kondon, C. Urano, Y. Kurihara, M. Nohara, and H. Takagi, J. Phys. Soc. Jpn. **69**, Suppl. B 139 (2000).
[32] A. N. Vasiliev, M. M. Markina, M. Isobe, and Y. Ueda, J. Magn. Magn. Mater. **300**, e375 (2006).
[33] A first-order transition is basically characterized by hysteresis and latent heat, both features making delicate the use of a relaxation technique to derive heat capacity. Keeping the standard analysis, special experimental parameters are required to get reliable data. In particular, we observed in the present case of MnV_2O_4 that artifacts can arise when using too large T rise and/or too short-time period in the heating/cooling process from which C is derived at each measuring point.
[34] T. A. Kaplan, Phys. Rev. **119**, 1460 (1960).
[35] N. Tristan, J. Hemberger, A. Krimmel, H. A. Krug von Nidda, V. Tsurkan, and A. Loidl, Phys. Rev. B **72**, 174404 (2005).